

to be important because, e.g., pair interactions are partially compensated at the fixed point by quadruple interactions of the same range.

In Table II we have listed the locus K_α^* of the fixed point in the various approximations together with the left eigenvector $r_\alpha = \varphi_\alpha^T / \varphi_{nn}^T$ belonging to λ_T . From this table one observes which interaction parameters are included and also that among the K_α^* the nearest-neighbor interaction stands out by a factor 15 over the other (negative) pair interactions, which again are a factor 4 larger than the four-spin interactions and many times larger than the six-spin interactions. Although the fixed point shifts notably, a lower approximation could very well be used as a guess for the fixed point of a higher approximation, indicating that the transformation does not develop singularities for larger and larger clusters at the fixed point (which is a basic assumption in the renormalization approach).

In Table I the values for λ_T , λ_H , and K_c are given and compared with the values for a triangular Ising system.⁴ The last approximation (seven cells symmetrically arranged) gives particularly accurate values, in our opinion, not only because it is the largest basic figure but also because its symmetry is the same as that of the lattice. On the basis of these λ_T and λ_H we find, e.g., the

critical exponents

$$\begin{aligned} \nu &= \ln l / \ln \lambda_T = 0.973, \\ \delta &= \ln \lambda_H / (2 \ln l - \ln \lambda_H) = 15.017, \end{aligned} \quad (10)$$

which should be compared with the exact values $\nu = 1$ and $\delta = 15$. The value of r_α may be compared with the coefficients giving the variation of $T_c(J)$ with J around the Ising system ($J_\alpha = 0$, $\alpha \neq nn$) obtained either analytically⁵ or numerically.⁶ Dalton and Wood⁶ find $r_{nnn} = 1.35$. Our rather high value of 1.607 could be lowered only a few hundredths by accounting for the curvature of the surface of criticality. One must conclude that longer-range forces than fit in our largest cluster play a role in determining r_α .

¹L. P. Kadanoff, *Physics* (Long Is. City, N.Y.) 2, 263 (1966).

²K. G. Wilson, *Phys. Rev. B* 4, 3174, 3189 (1971).

³A more detailed discussion can be found in Th. Nijmeijer and J. M. J. van Leeuwen, to be published.

⁴R. M. F. Houtappel, *Physica* (Utrecht) 16, 425 (1950).

⁵P. T. Herman and J. R. Dorfman, *Phys. Rev.* 176, 295 (1968); *J. Math. Phys.* (N.Y.) 5, 1009 (1964).

⁶N. W. Dalton and D. W. Wood, *J. Math. Phys.* (N.Y.) 10, 1271 (1969).

Tricritical Lines in Metamagnets

C. Vettier

Institut Laïe-Langevin, 38042 Grenoble Cedex, France

and

H. L. Alberts* and D. Bloch

Laboratoire de Magnétisme, 38042 Grenoble Cedex, France

(Received 26 September 1973)

Measurements of the magnetization of FeBr_2 and FeCl_2 as a function of magnetic field, temperature, and hydrostatic pressure establish lines of tricritical points T_{3c} with slopes $(T_{3c})^{-1} dT_{3c}/dP = -0.025$, $+0.021$, and $+0.040 \text{ kbar}^{-1}$ for the low- and high-pressure phases of FeCl_2 and for FeBr_2 , respectively. The variation of the tricritical transition with pressure should provide sensitive tests of theories relating interaction constants in the Hamiltonian to tricritical behavior in magnetic systems.

Considerable interest has been aroused recently by the existence of tricritical points, which involve the meeting of a line of second-order transitions with a line of first-order transitions.¹ Metamagnets such as FeCl_2 and FeBr_2 ² provide typical examples of such tricritical points; other

examples are the two-fluid critical mixing point in He^3 - He^4 , the order-disorder transitions in NH_4Cl and NH_4Br , thin superconducting films, and the metamagnet dysprosium aluminum garnet. There are two levels to the problem of tricritical points. The first is understanding their

existence and their variation with external conditions such as applied pressure, and the second involves the critical exponents close to the tricritical point. As a consequence of the difficulty in getting a sufficiently uniform magnetic field nothing can be said about the second problem from our magnetization measurements.

FeCl_2 and FeBr_2 possess, respectively, at atmospheric pressure a hexagonal structure of the CdCl_2 type (with three Fe atoms per unit cell) and of the CdI_2 type (with one Fe atom per unit cell). FeCl_2 has the additional feature that a change in crystal structure occurs at a pressure of a few kilobars (2 kbar at low temperatures), from the low-pressure phase $(\text{FeCl}_2)_I$ to a high-pressure phase $(\text{FeCl}_2)_{II}$ which, it has been suggested,³ is of the CdI_2 type. FeBr_2 and $(\text{FeCl}_2)_I$ can be considered as composed of hexagonal sheets of Fe^{2+} spins, which at low temperatures are ferromagnetically aligned along the hexagonal c axis, whereas successive sheets are stacked antiferromagnetically.⁴

When an internal magnetic field H (that is, the external field H_{appl} less a demagnetizing field) is directed along the c axis, then, at a threshold field H_c , a transition occurs to a paramagnetic phase of high magnetic moment. At a given pressure P this transition is of first order (or metamagnetic) from temperatures $T=0$ to T_{3c} and of second order (or Néel transition) between T_{3c} and $T_N(H=0)$, where $T_N(H=0)$ is the Néel temperature in the absence of an applied magnetic field (Fig. 1).

One can expect to determine, from experiments performed at various pressures, a tricritical line in H, T, P space. A rather complete knowledge of the high-pressure magnetic behavior of these compounds is needed in order to relate the values of the tricritical parameters to the relevant magnetic parameters such as exchange and anisotropy coefficients. This is why we have determined completely, under various high-pressure conditions, the first-order line and the second-order line which meet at the tricritical point.

The magnetization M of single crystals of FeBr_2 and FeCl_2 has been determined as a function of field up to 50 kOe, pressure up to 6.5 kbar, and temperature between 4.2 and 30 K. The experimental techniques have been described elsewhere.⁵ Small disks of 5 mm diameter, which have been cut perpendicularly to the hexagonal c axis, have been stacked together in order to get cylinders of 10 mm length. The bulk samples are thus not of ellipsoidal shape, and the internal

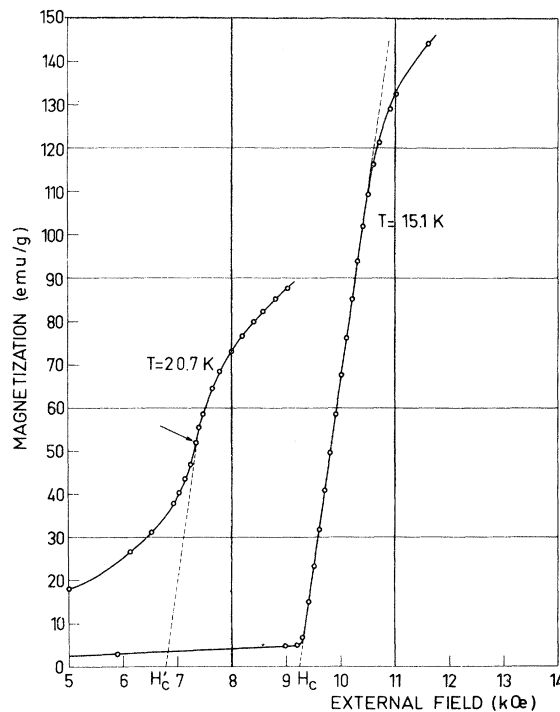


FIG. 1. Magnetization M versus applied field H_{appl} for FeCl_2 at atmospheric pressure at $T=0$ K. Below the tricritical temperature $T_{3c}=20.3$ K, one observes a metamagnetic transition where the slope of $M(H_{\text{appl}})$ is due to the demagnetizing field only. The threshold field H_c of the metamagnetic transition is determined as indicated. That of the second-order (continuous) antiferromagnetic-paramagnetic transition is defined from the slope discontinuity of the $M(H_{\text{appl}})$ curve.

magnetic field tends to be, to some extent, inhomogeneous.

Typical curves of magnetization as a function of external magnetic field for different temperatures at constant pressure are shown in Fig. 1. At the first-order transition, it is assumed that the slope in the magnetization curve is due to demagnetizing effects.² Above the tricritical temperature, the critical point is defined from the point where a slope discontinuity appears.⁵ In order to convert these data from external field to internal field it is necessary to make some assumption about the demagnetizing field. We assume that we may define a demagnetizing factor from the magnetization curves at low temperatures; it is further assumed that the demagnetizing factor does not vary in the second-order region.

At low temperature, below the tricritical point, the first-order threshold field is defined within a few oersteds. The inhomogeneity in the inter-

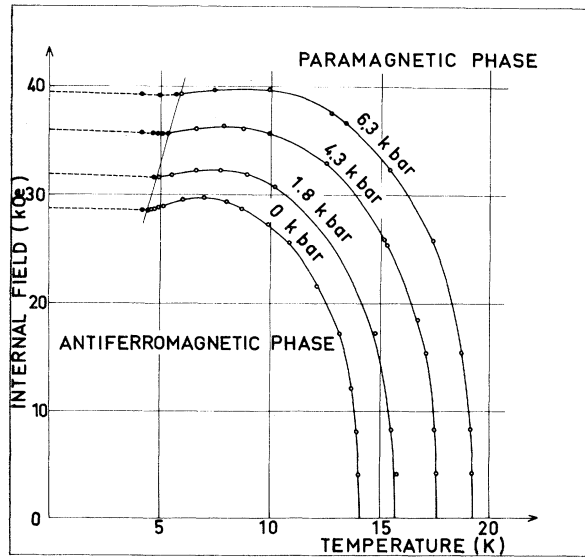


FIG. 2. Magnetic phase diagrams of FeBr₂. Full straight line separates regions where the antiferromagnetic transition is of first order (at low temperature) and second order (at high temperature).

nal field gives rise to a nonlinear magnetization-external-field ($M-H_{app}$) relationship only at the beginning or at the end of the field range where antiferromagnetism and paramagnetism occur simultaneously. Above the tricritical point, up to the zero-field Néel temperature, the threshold field is defined within a few tens of oersteds. The experimental situation is difficult to describe with good accuracy in the neighborhood of the tricritical temperature. In the range $T_{3c} \pm 0.5$ K, it is more and more difficult to define the order of the magnetic transition as the temperature approaches T_{3c} . We define the tricritical temperature at a given pressure as the temperature for which dM/dH_{app} at the antiferromagnetic-paramagnetic transition changes rapidly. We then estimate the

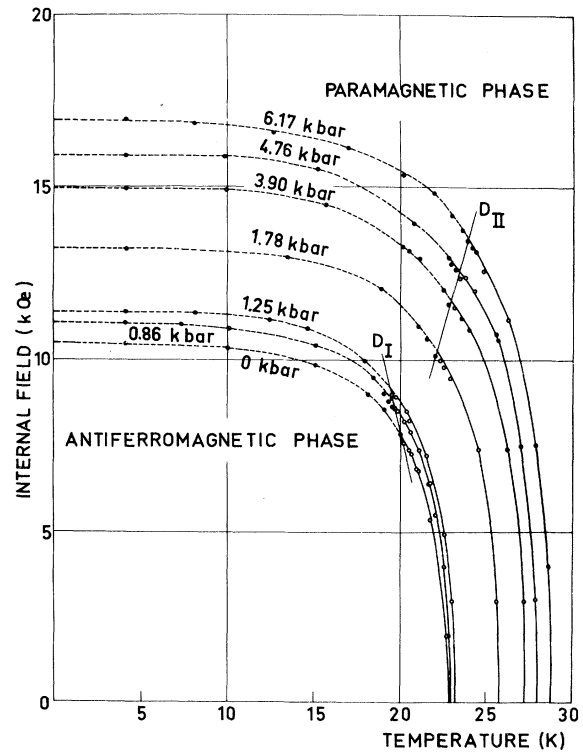


FIG. 3. Phase diagrams of FeCl₂. A crystallographic phase change occurs at approximately 2 kbar. Full lines D_I and D_{II}, which are associated to the low-(FeCl₂)_I and high-pressure (FeCl₂)_{II} phases, separate regions where the antiferromagnetic-paramagnetic transition is of first order (at low temperature) and second order (at high temperature).

accuracy of the tricritical temperature to be ± 0.1 K and the accuracy of the critical field to be ± 0.1 kOe.

Using this procedure, the curves of internal transition field versus temperature are obtained at different pressures. The measurements established tricritical lines in the H, T, P space for

TABLE I. Threshold field H_c , Néel temperature T_N , tricritical temperature T_{3c} , tricritical field H_{3c} , and their pressure derivatives for FeBr₂ and the low-pressure phases (I and II) of FeCl₂.

	$H_c(T=4.2 \text{ K}, P=0)$	$\frac{10^2 dH_c}{H_c dP}$ ($T=4.2 \text{ K}$) (kbar ⁻¹)	$T_N(H=0, P=0)$ (K)	$\frac{10^2 dT_N}{T_N dP}$ (kbar ⁻¹)	$T_{3c}(P=0)$ (K)	$\frac{10^2 dT_{3c}}{T_{3c} dP}$ (kbar ⁻¹)	$H_{3c}(P=0)$ (kOe)	$\frac{10^2 dH_{3c}}{H_{3c} dP}$ (kbar ⁻¹)
FeBr ₂	28.8	5.9	14.1	5.8	4.6	4.0	28.5	5.8
(FeCl ₂) _I	10.45	7.0	22.9	1.1	20.3	-2.5	7.55	14.3
(FeCl ₂) _{II}	11.68 ^a	7.3	24.75 ^a	2.75	21.15 ^a	2.1	8.7 ^a	8.8

^a Extrapolated to $P=0$.

FeBr_2 , $(\text{FeCl}_2)_I$, and $(\text{FeCl}_2)_{II}$. The magnetic phase diagram of FeBr_2 , which is shown in Fig. 2, exhibits changes in the slopes of the transition lines at the tricritical point, as reported at 1 atm by Fert *et al.*² For the two structural phases of FeCl_2 , Fig. 3, a small change in slopes has been observed, but it might be associated with inhomogeneities of the internal magnetic field.

FeCl_2 provides a system in which the tricritical point can be studied in two different environments without change in composition: In the low-pressure phase $(\text{FeCl}_2)_I$ the tricritical temperature decreases with applied pressure, but in the high-pressure phase $(\text{FeCl}_2)_{II}$ it increases as it does in FeBr_2 .

The zero-pressure values for threshold field, Néel temperature, tricritical temperature, and field and their pressure derivatives are given in Table I. The 1-atm values are in satisfactory agreement with those given by previous experiments.²

The variations of exchange and anisotropy can be deduced from these and other measurements such as antiferromagnetic resonance⁶ or perpendicular susceptibility⁷ under pressure. By relating these variations to the tricritical lines the validity of theories of phase transitions can be tested. Elastic and inelastic neutron scattering studies in $(\text{FeCl}_2)_{II}$ and compressibility measurements are now in progress in order to use volume rather than pressure basis. A complete discussion of these results will be reported later.

We are grateful to Dr. R. J. Birgeneau, Dr. P.

Carrara, Dr. A. Fert, Dr. D. B. McWhan, and Dr. W. D. Yelon for fruitful discussions.

*Permanent address: Department of Physics, Rand Afrikaans University, Johannesburg, South Africa.

¹See for general references R. B. Griffiths, *Phys. Rev. B* **7**, 545 (1973); L. S. Schulman, *Phys. Rev. B* **7**, 1960 (1973); F. J. Wegner and E. K. Riedel, *Phys. Rev. B* **7**, 248 (1973); L. Benguigui, *Phys. Lett.* **40A**, 153 (1972); A. M. Goldman, *Phys. Rev. Lett.* **30**, 1038 (1973).

²See for general references I. S. Jacobs and P. E. Lawrence, *Phys. Rev.* **164**, 866 (1967). Other references: R. P. Kenan, R. E. Mills, and C. E. Campbell, *J. Appl. Phys.* **40**, 1027 (1969); P. Carrara, J. de Gunzbourg, and Y. Allain, *J. Appl. Phys.* **40**, 1035 (1969); R. J. Birgeneau, W. B. Yelon, E. Cohen, and J. Makovsky, *Phys. Rev. B* **5**, 2607 (1972); W. B. Yelon and R. J. Birgeneau, *Phys. Rev. B* **5**, 2615 (1972); A. R. Fert, P. Carrara, M. C. Lanusse, G. Mischler, and J. P. Redoules, *J. Phys. Chem. Solids* **34**, 223 (1973).

³A. Narath and J. E. Schirber, *J. Appl. Phys.* **37**, 1124 (1966).

⁴A. Herpin and P. Meriel, *Colloque National de Magnétisme, Strasbourg, 1957* (Centre National de la Recherche Scientifique, Paris, 1958), p. 105; M. K. Wilkinson, J. W. Cable, E. D. Wollan, and W. C. Koehler, *Phys. Rev.* **113**, 497 (1959).

⁵J. Beille, H. L. Alberts, H. Bartholin, D. Bloch, and C. Vettier, *C.R. Acad. Sci., Ser. B* **275**, 719 (1972); C. Vettier, H. L. Alberts, J. Beille, and D. Bloch, *C.R. Acad. Sci., Ser. B* **275**, 915 (1972).

⁶K. C. Johnson and A. J. Sievers, *Phys. Rev. B* **7**, 1081 (1973).

⁷C. Vettier and D. Bloch, to be published.

Persistence of the Stoner Splitting in Metallic Ferromagnets above T_c †

J. B. Sokoloff

Department of Physics, Northeastern University, Boston, Massachusetts 02115

(Received 13 August 1973)

Recent neutron-diffraction experiments by Mook, Lynn, and Nicklow, as well as previous photoemission experiments by Pierce and Spicer, provide evidence that the Stoner band splitting in nickel might not go to zero at T_c , as it does in conventional band theory of magnetism. It will be shown that the persistence of such splitting in the paramagnetic regime can be explained quite naturally within the framework of the random-phase-approximation theory of spin fluctuations.

Recently Mook, Lynn, and Nicklow observed using inelastic neutron diffraction¹ the rapid reduction of the spin-wave scattering intensity on entering the stoner continuum in nickel as a function of temperature. They found that the lower edge of the Stoner continuum did not appear to come down as they raised the temperature through the Curie temperature, as Stoner-Hartree-Fock theory would predict. This result lends support to the photoemission results of Pierce and Spicer,² which also imply that no